

Electronic Supporting Information

Singlet oxygen oxidations in homogeneous continuous flow using a gas-liquid membrane reactor

Antonia Kouridaki and Kevin Huvaere

EcoSynth NV, Industrielaan 12, B-9800 Deinze, Belgium

e-mail: khuvaere@ecosynth.be

Table of contents

1	General information	2
2	Reactor setup.....	2
3	Validation of the operational system	3
	2.1 Oxygen feed	3
	2.2 Temperature of the photoreactor	5
	2.3 LED source emission spectrum	5
4	General experimental procedure	6
5	Spectroscopic data.....	9
	5.1 NMR data.....	9
	5.2 Copies of ¹ H-NMR, ¹³ C-NMR and HMBC spectra	11
6	Chromatographic data.....	16
7	References	19

1 General information

All commercially available compounds and solvents were used without further purification. Solvents (methanol, dichloromethane, acetonitrile, ethyl acetate, petroleum ether) were purchased from VWR (Leuven, Belgium). Rose Bengal, benzylamine (99%), α -terpinene (90%), citronellol (95%), thioanisole (99%) and methyl phenyl sulfoxide (98%) were purchased from Acros Organics (Geel, Belgium). Ethyl 3-(2-furyl)propanoate (98%) and sodium borohydride were purchased from Sigma-Aldrich (Machelen, Belgium), methylene blue from Fluka (Machelen, Belgium), tetraphenylporphyrin and methyl phenyl sulfone (97%) from TCI (Zwijndrecht, Belgium).

NMR spectra were recorded on a Bruker 300 MHz spectrometer, typically using deuterated chloroform as solvent and with TMS as internal reference. The following abbreviations are used to explain the multiplicities: s = singlet, d = doublet, t = triplet, q = quartet, m = multiplet, br = broad.

Conversions were determined by GC-FID analysis, using decane as internal standard. GC-FID analyses were run on an Agilent 7890 gas chromatograph (equipped with a 100% dimethylpolysiloxane Varian VF-1ms column; 30 m \times 250 μ m \times 1 μ m) with detection by flame ionization detection. Following settings were applied: start at 60°C and keep for 1 min, mount to 300°C at 35°C/min, keep for 1 min and raise to 320°C at 20°C/min, the final temperature which is kept for 2 min. Injection (1 μ L) occurred in split mode (20:1) at a temperature of 250°C. Hydrogen was used as carrier gas at a flow of 1.0 mL/min.

Product formation was monitored with GC-MS and TLC analysis. For the GC-MS analysis, reaction mixtures were filtered through a short path of charcoal and celite in order to remove the photosensitizer. Analyses were run on an Agilent 7890 gas chromatograph (equipped with a non-polar 5%-phenyl-methylpolysiloxane (Agilent HP5-MS) column; 30 m \times 250 μ m \times 0.25 μ m). Detection occurred by a quadrupole mass spectrometer (Agilent 5975 C) operating in electron impact ionization mode scanning between 40 and 750 amu. A short temperature program in which temperature was ramped from 70°C (keep for 1 min) to 280°C at 45°C/min to stay at the final temperature for 4.5 minutes. Injection (1 μ L) occurred in split mode (10:1) at a temperature of 280°C. Helium was used as carrier gas at a flow of 1 mL/min. TLC analysis was carried out using silica gel on Al foils. An acidic mixture of phosphomolybdic acid cerium (IV) sulfate was used as color reagent and UV light as visualizing agent.

2 Reactor setup

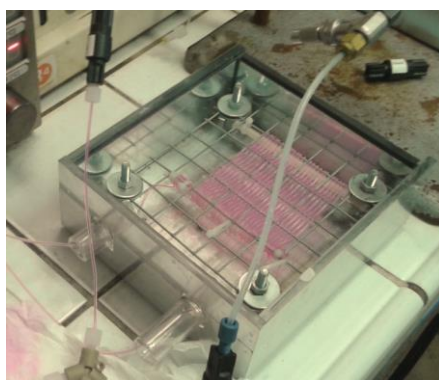
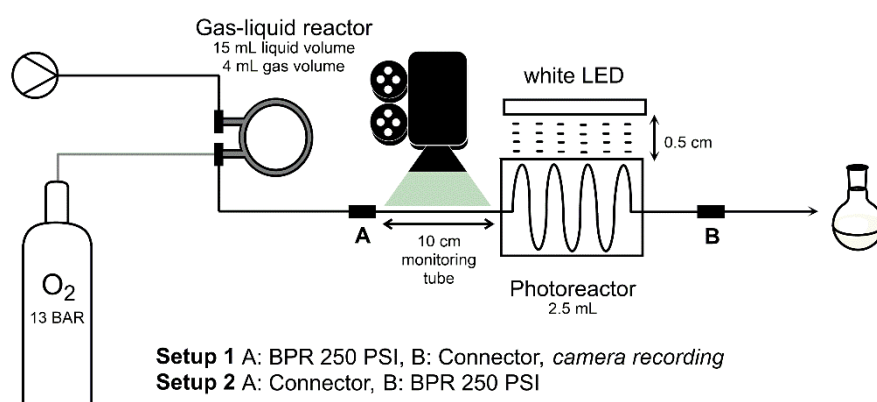


Fig. S1 Picture of the custom-built photoreactor as used in this work (here in use with rose Bengal as sensitizing agent). LED lamp, normally placed on top, is removed to show tube pattern.

A RS-200 – Automated Control module from Vapourtec (Suffolk, UK) was used to pump substrate solutions into the gas-liquid reactor (part number 50-1241, also from Vapourtec), which is directly connected to a standard two-stage gas pressure regulator mounted on a gas bottle for oxygen supply. During all experiments pressure of oxygen was maintained at 13 bar, obviously except for experiments evaluating effect of pressure. For temperature control, the reactor was installed in a special insulated glass manifold that permits rapid temperature changes by circulating heated air. Upper limit operating conditions of the gas-liquid reactor are 150 °C for membrane temperature, 30 bar gas pressure, and 30 bar liquid pressure. Depending on the solvent used, there is a minimum pressure requirement to prevent solvent boiling at elevated temperatures. Accordingly, a 250 psi back pressure regulator (BPR) was installed which allows pressurization of the entire system. As such, operating temperatures ranged up to 110 °C for MeOH and MeCN, while 90 °C was reached for the lower boiling DCM. The oxygen saturated solutions leaving the gas-liquid reactor were cooled to ambient temperature by a post cooling coil and transferred to the photoreactor, which consisted of fluorinated ethylene propylene tubing (FEP, 2.5 mL or 6.0 mL, internal diameter 0.8 mm, outer diameter 1.6 mm) wrapped on a metal frame (8×10 cm) (Fig. S1). A 20 Watt LED lamp (type 1301, Profile) or a 50 Watt LED lamp (260, PowerPlus), positioned at a distance of 0.5 cm from the photoreactor was used for the irradiation of the reaction mixtures. Photooxygenations were carried out under **heterogeneous conditions** (i.e., a biphasic flow regime) when the BPR was placed in between gas-liquid reactor and photoreactor (Fig. S2, setup 1). A similar setup, but with camera mounted for observation of gas bubble formation in a 10 cm monitoring tube placed after the BPR was used for assessing oxygen supply. On the other hand, setup 2, with BPR at the photoreactor exit, was used for photooxygenation reactions under pressurized, **homogeneous conditions** (Fig. S2, setup 2).



*Fig. S2 Detailed representation of the operating system: **setup 1** with BPR at the inlet of the photoreactor for monitoring oxygen supply (or for photooxidations under heterogeneous flow regime) and **setup 2** with BPR at the exit for homogeneous flow in the photoreactor.*

3 Validation of the operational system

3.1 Oxygen feed

Oxygen supply in MeOH, MeCN, and DCM under varying temperatures and flows was investigated in a slightly modified setup, i.e. setup 1 with photoreactor being superfluous and the BPR being installed at the gas-liquid reactor exit. Downstream of the BPR in a 10 cm calibrated FEP tube, number and length of oxygen segments released from the solvent were monitored during a 60 seconds timeframe recorded by digital camera (Fig. S3). Quantitative determination of the total amount of oxygen that

was initially dissolved, was carried out as follows. Individual gas segment length was summed to total length per minute and converted to the corresponding volume, using:

$$V = \pi r^2 h$$

where V = volume of O_2 (mL), r = internal radius of tube (0.04 cm), h = total length of O_2 segments observed (cm).

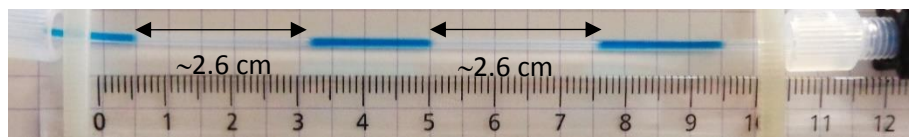


Fig. S3 Measurement of oxygen segments in MeOH at a flow rate of 0.25 ml min^{-1} , at 50°C .

For example, for a flow rate of 0.25 mL min^{-1} , at 50°C membrane temperature, 26 bubbles with average 2.6 cm length were generated giving 67.6 cm total length (h), corresponding to an oxygen volume of $0.338 \text{ mL min}^{-1}$. Volume of oxygen was converted to the corresponding moles delivered in the solution per minute using the ideal gas law:

$$n = \frac{PV}{RT}$$

where n = moles of O_2 , $P = 1 \text{ atm}$ ($\sim 1.01 \text{ bar}$, assuming back pressure at end of pipe is negligible), V = volume of O_2 (mL), $R = 82.06 \text{ mL atm mol}^{-1} \text{ K}^{-1}$, $T = 298 \text{ K}$. Using MeOH as solvent in the example, 1.38×10^{-5} moles of oxygen are introduced per minute corresponding to 55.3 mM (C_{O_2}). Given that saturated MeOH contains 1.99 mM of oxygen at 1 atm at ambient temperature,¹ total concentration of oxygen (C_{tot}) was calculated to be 57.3 mM (Table S1).

Table S1 Calculated results for the supply of oxygen in MeOH at increasing liquid flow rates, at constant membrane temperature of 50°C .

Flow rate (mL min ⁻¹)	h (cm min ⁻¹)	V (mL min ⁻¹)	C_{O_2} (mM)	C_{tot} (mM)
0.25	67.6	0.338	55.3	57.3
0.5	78.8	0.396	32.4	34.4
0.75	83.4	0.419	22.8	24.8
1.0	81.4	0.409	16.7	18.7

Table S2 Calculated results for the supply of oxygen in different solvents at elevating temperatures for a flow rate of 1.0 mL min^{-1} .

Solvent	T ($^\circ\text{C}$)	h (cm min ⁻¹)	V (mL min ⁻¹)	C_{O_2} (mM)	C_{tot} (mM)
MeOH	25	36.4	0.183	7.5	9.5
	50	81.4	0.409	16.7	18.7
	110	233.5	1.173	48.0	50.0

Table S2 Continued.

Solvent	T (°C)	h (cm min ⁻¹)	V (mL min ⁻¹)	C _{O₂} (mM)	C _{tot} (mM)
MeCN	25	57.2	0.287	11.7	14.4
	50	88.7	0.446	18.2	20.8
	110	266.2	1.338	54.7	57.3
DCM	25	119.3	0.599	24.5	33.3
	50	218.5	1.098	44.9	57.3
	90	450.8	2.266	92.6	101.5

Similarly, the amount of oxygen delivered in MeCN and DCM was determined for a liquid flow rate of 1.0 mL min⁻¹ at varying temperatures (Table S2), taking into account the amount of dissolved gas under ambient conditions (1 atm) which is 2.6 mM and 8.8 mM for MeCN and DCM, respectively.^{1,2}

3.2 Temperature of the photoreactor

In order to confirm that increasing temperatures of the reactor membrane do not affect kinetics of subsequent oxidations in the photoreactor, efficiency of the post cooling device installed inside of the gas-liquid reactor was investigated. For this purpose, a solution of citronellol (50.0 mM) in MeCN containing 0.1 mM MB as photosensitizer, was photooxidized under homogeneous conditions. To ensure sufficient cooling, the tube connecting gas-liquid reactor and photoreactor was submerged in a water bath. The experiment was repeated in the absence of bath, thus fully relying on the post cooling device for heat dissipation. As only very minor changes in conversion for the two experiments were observed (Table S3), a potential effect of membrane temperature on photoreactions was refuted.

Table S3 Investigation of post cooling efficiency of gas-liquid reactor in photooxidation of citronellol (50.0 mM in MeCN containing 0.1 mM MB).

Experimental conditions	Additional cooling*	Conversion
Flow rate: 1.0 mL min ⁻¹ T (membrane): 90 °C	yes	86.4 %
Volume of photoreactor: 6 mL LED source: 50 W	no	88.6 %

* Cooling of the tube connecting gas-liquid reactor exit and photoreactor entry

3.3 LED source emission spectrum

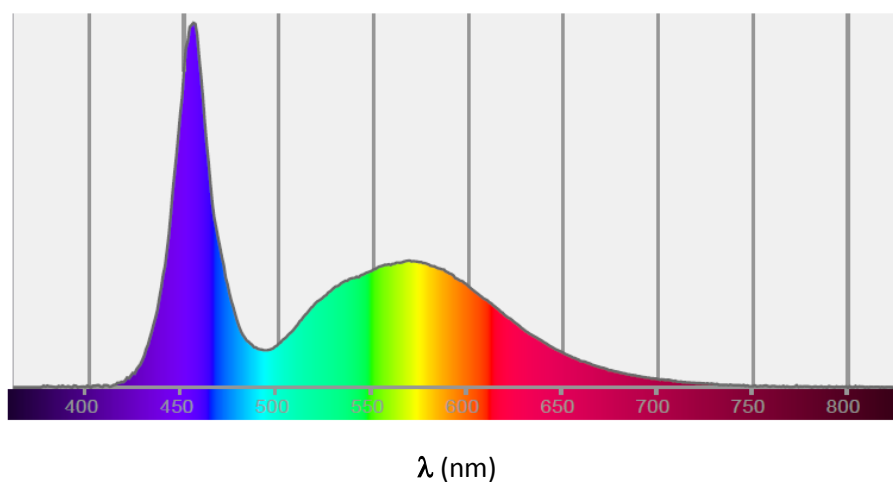
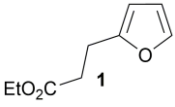
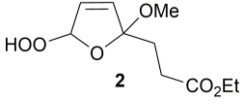
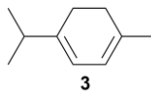
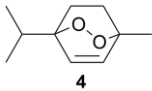
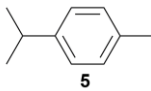
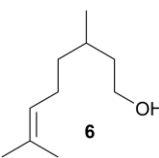
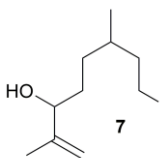
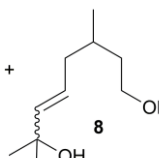
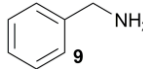
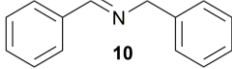
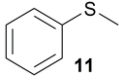
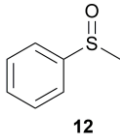


Fig. S4 Emission spectrum of the 20 W white LED lamp

For the majority of experiments, a commercially available, 20 W white LED lamp was used. According to detailed assessment of irradiation parameters (using a LightSpion, Viso Systems, Copenhagen, Denmark), color temperature was 8713 K (warm white) which was produced by an intense blue component, in combination with emissions of red and green light as concluded from spectral measurements (Fig. S4). It is worth noting that beyond 700 nm, no emission is recorded hence no heat (infrared light) is transferred to illuminated samples.

4 General experimental procedure

Table S4 Typical reaction conditions of various substrates and isolated yields.

Entry ^a	Substrate	Product	Photosens., Solvent	Flow rate (mL min ⁻¹)	T (°C)	Yield (%)
1			MB, MeOH	0.5	70	90
2		 + 	RB, MeCN	0.5	90	90
3		 + 	MB, MeCN	0.5	90	94
4			MB, MeCN	0.25	100	57
5			MB, MeOH	0.5	70	85 ^b

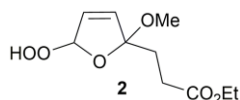
^a Reaction mixtures of entries 1-4 were irradiated in a 2.5 mL photoreactor using a 20 W lamp, while reaction mixture of entry 5 was irradiated in a 6 mL photoreactor, using a 50 W lamp. ^b Yield was determined by GC-FID analysis, using internal standardization and calibration curve constructed from authentic methyl phenyl sulfoxide reference material.

Solutions of compounds **1**, **3**, **6**, **9** and **11** (50 mM) containing the appropriate photosensitizer (0.1 mM) were irradiated in homogeneous flow under the conditions described in Table S4. Reaction mixtures (100 mL) were collected after 50 mL of the solutions were first expelled (entries 1-4). The mixtures were concentrated *in vacuo* and the residues (entries 1, 2, 4) were purified by flash column chromatography (silica gel, petroleum ether/EtOAc 1:1 for entry 1, 20:1 for entry 2 and silica gel basified with triethylamine, petroleum ether/EtOAc 10:1 for entry 4). In the case of entry 3, the residue was dissolved in MeOH (30 mL) and NaBH₄ (1.0 eq, 5 mmoles, 189 mg) was added. After stirring for 1 hour at RT, reaction mixture was partly concentrated *in vacuo*. Then Et₂O (20 mL) was added and the mixture was washed with H₂O (2×10 mL). Drying (MgSO₄) of the organic phase, filtration and evaporation of the solvent afforded crude mixture that was purified by flash column chromatography (silica gel, petroleum ether/EtOAc 1:1). In the case of entry 5, product formation was characterized by comparing retention time in GC-FID analysis with retention time of authentic reference material (i.e., methyl phenyl sulfoxide **12**). Structure identification was confirmed by GC-MS, for which electron impact mass spectra for the product were compared with corresponding reference spectrum. A minor impurity, according to analogous structure elucidation attributed to methyl phenyl sulfone (MPS), was found to be present in very low quantities (≤ 1 %, molar ratio). The latter was concluded after spiking of minute, known quantities of MPS to **12**, followed by calculating

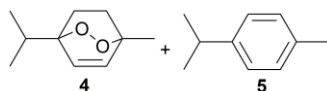
peak area ratios which were compared to the peak area ratio in the product mixture (See paragraph 6, p.16 for details).

5 Spectroscopic data

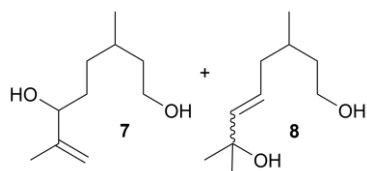
5.1 NMR data



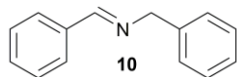
Ethyl 3-(5-hydroperoxy-2-methoxy-2,5-dihydrofuran-2-yl)propionate (2). (1.04 g, 90.0%); ^1H NMR (300 MHz, CDCl_3): δ = 9.14 (s, -OOH), 6.00 (m, 3H), 4.11 (q, J = 7.2 Hz, 2H), 3.20 (s, 3H), 2.36 (m, 2H), 2.16 (m, 2H), 1.24 (t, J = 7.2 Hz, 3 H) ppm; ^{13}C NMR (300 MHz, CDCl_3): δ = 173.3, 135.8, 127.5, 114.0, 109.4, 60.5, 50.8, 33.8, 29.0, 14.2 ppm.



1-Methyl-4-(1-methylethyl)-2,3-dioxabicyclo[2.2.2]oct-5-ene (ascaridole, 4), 1-methyl-4-(propan-2-yl)benzene (*p*-cymene, 5).³ (Inseparable mixture of 4:5 in 1:0.1 ratio, 735 mg, 90.4% taking into account the purity of the product and the purity of the starting material); ^1H NMR (300 MHz, CDCl_3): δ = 7.11 (s, 4H, 5), 6.50 (d, J = 8.4 Hz, 1H, 4), 6.41 (d, J = 8.4 Hz, 1H, 4), 2.87 (m, 1H, 5), 2.31 (s, 3H, 5), 2.02 (m, 2H, 4), 1.90 (m, 1H, 4), 1.53 - 1.50 (m, 2H, 4), 1.37 (s, 3H, 4), 1.23 (d, J = 6.9 Hz, 6H, 5), 1.00 (d, J = 6.9 Hz, 6H, 4), 0.98 (s, 3H, 4) ppm; ^{13}C NMR (4, 300 MHz, CDCl_3): δ = 136.4, 133.0, 79.8, 74.4, 32.1, 29.5, 25.6, 21.4, 17.2.



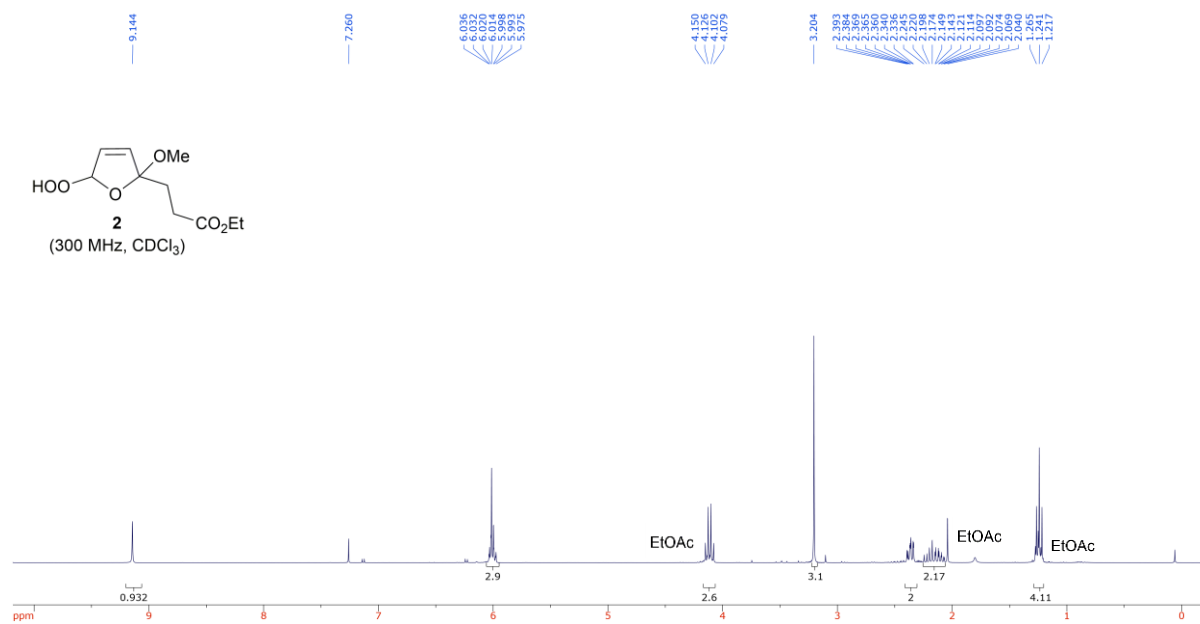
3,7-Dimethyl-5-octene-1,7-diol (7), 3,7-dimethyl-7-octene-1,6-diol (8).^{3,4} (Inseparable 1:1 mixture of 2 regio-isomers as determined by NMR, 770 mg, 94.2% taking into account the purity of the starting material); ^1H NMR (300 MHz, CDCl_3): δ = 5.59 (m, 2H, 8), 4.92 (m, 1H, 7), 4.83 (m, 1H, 7), 4.03 (t, J = 6.5 Hz, 1H, 7), 3.67 (m, 2H for 7 plus 2H for 8), 2.03 (m, 1H, 8), 1.90 (m, 1H, 8), 1.71 (s, 3H, 7), 1.67 - 1.50 (m, 6H plus 4OH), 1.47 - 1.24 (m, 4H), 1.30 (s, 6H, 8), 0.90 (m, 3H for 7 plus 3H for 8) ppm; *Signals at 4.92 ppm from diol 7 (corresponding to 1 H) and at 2.03 ppm from diol 8 (corresponding to 1 H) were used to determine ratio between both isomers.*³ ^{13}C NMR (300 MHz, CDCl_3): δ = 147.6, 147.5, 139.6, 125.2, 111.2, 110.9, 76.3, 76.0, 70.7, 61.0, 39.7, 39.3, 32.7, 32.6, 32.2, 32.1, 29.9, 29.8, 29.7, 29.5, 29.3, 19.6, 19.5, 17.6, 17.4 ppm.



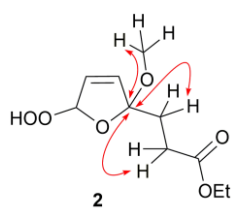
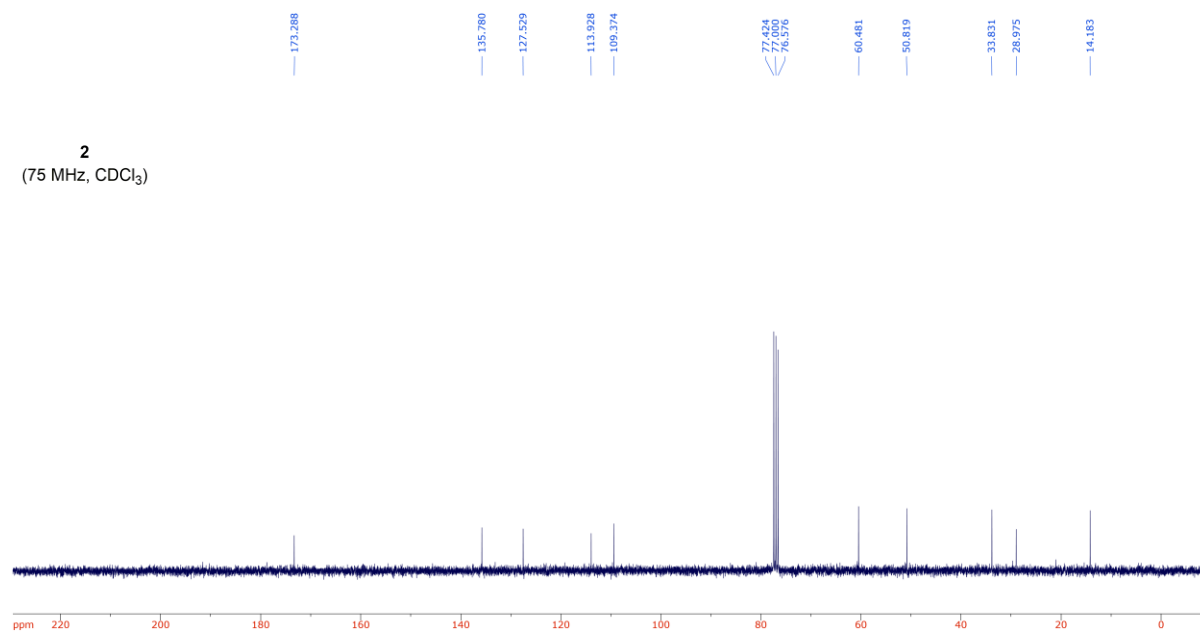
(E)-(Phenylmethylidene)(benzyl)amine (10).⁵ (556 mg, 57.0%)

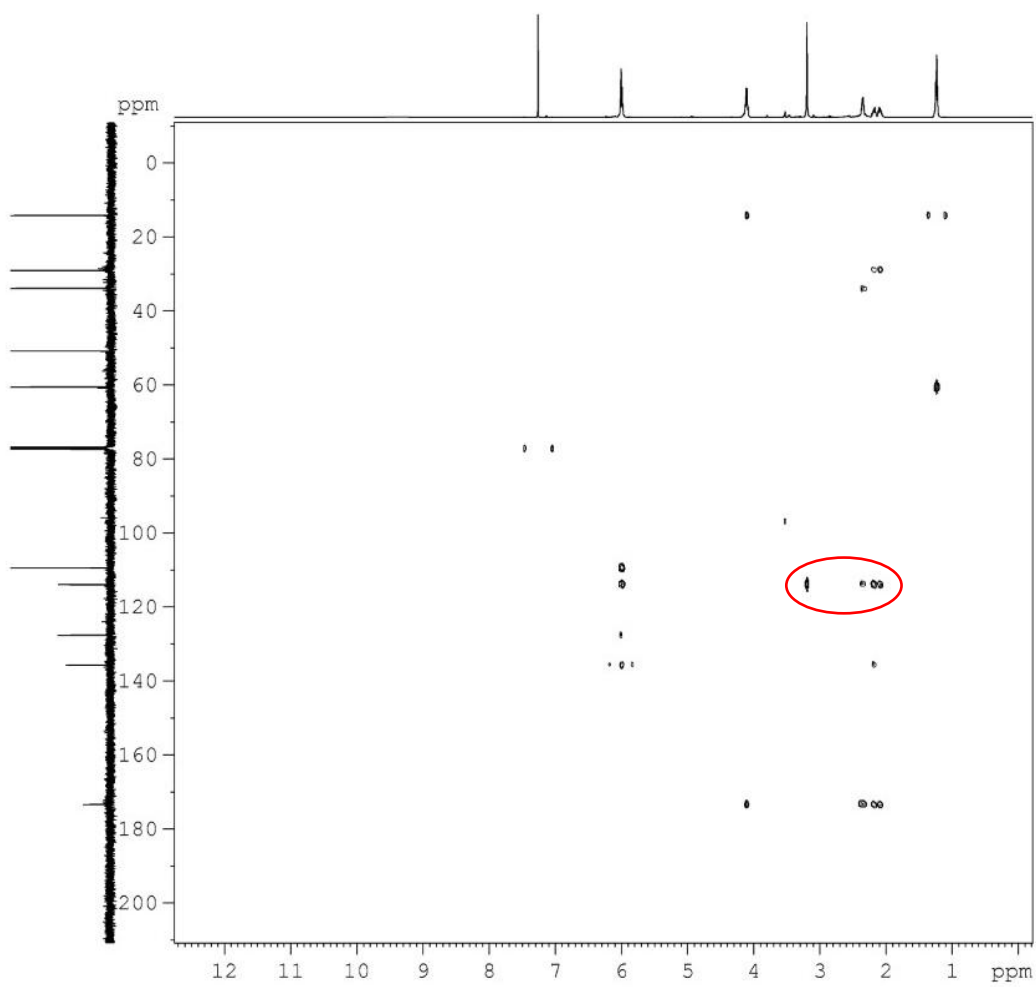
¹H NMR (300 MHz, CDCl₃): δ = 8.41 (s, 1H), 7.79 (m, 2H), 7.43 (m, 3H), 7.35 (m, 4H), 7.30 - 7.24 (m, 1H), 4.84 (s, 2H) ppm; ¹³C NMR (300 MHz, CDCl₃): δ = 162.0, 139.2, 136.1, 130.7, 128.6, 128.5, 128.0, 127.0, 65.0 ppm.

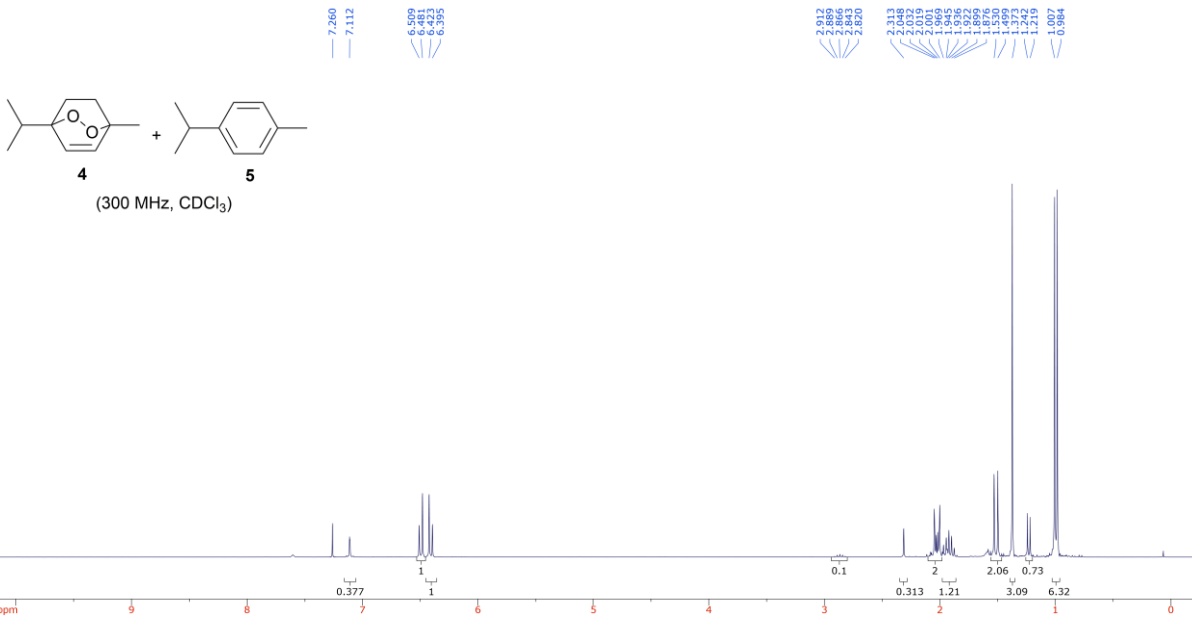
5.2 Copies of $^1\text{H-NMR}$, $^{13}\text{C-NMR}$ and HMBC spectra



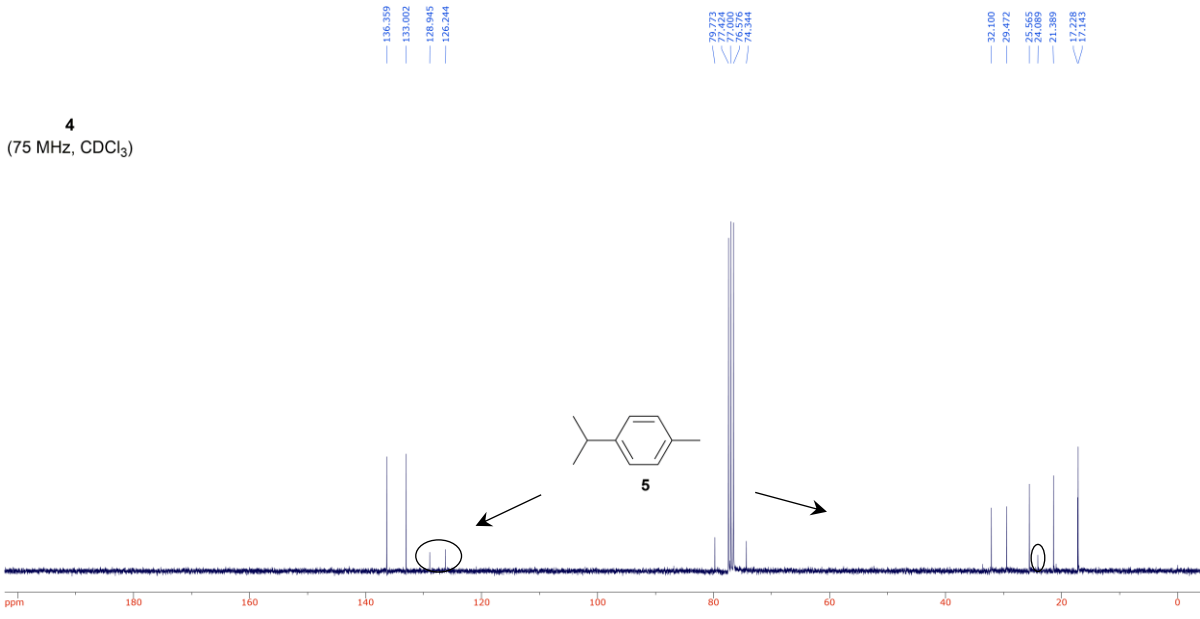
2
(75 MHz, CDCl_3)

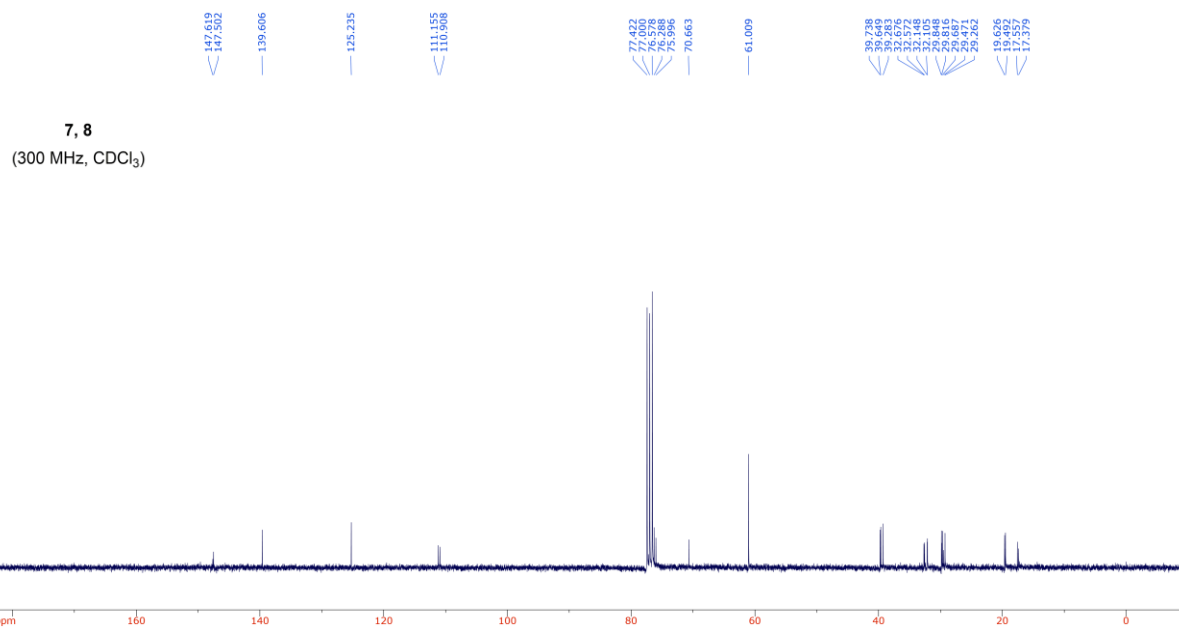
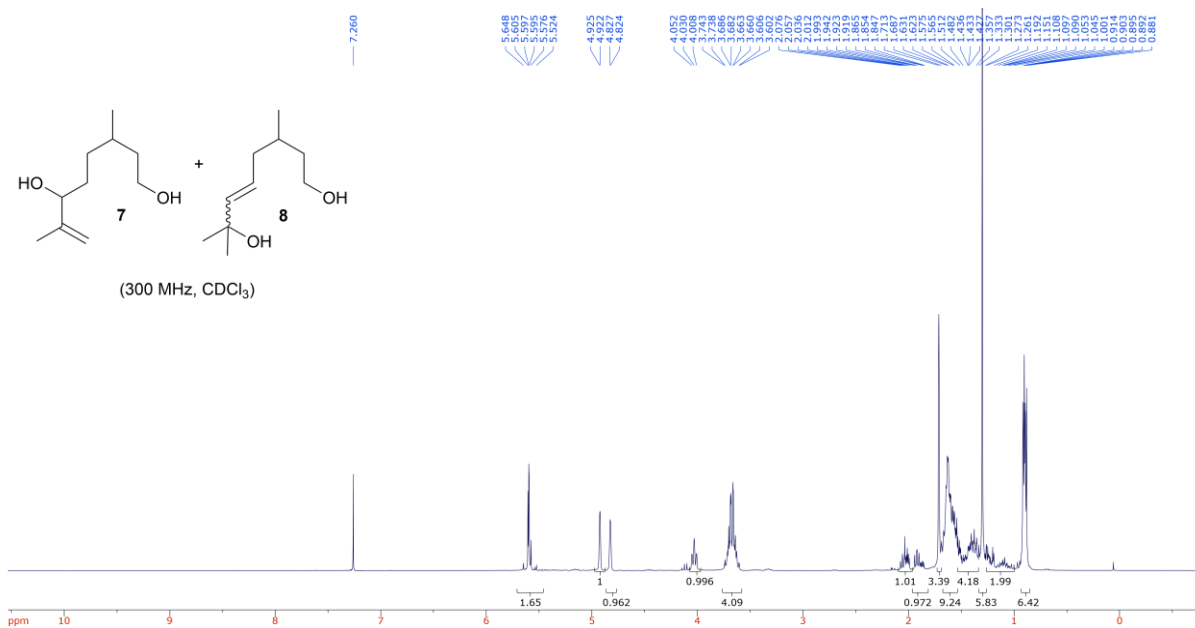


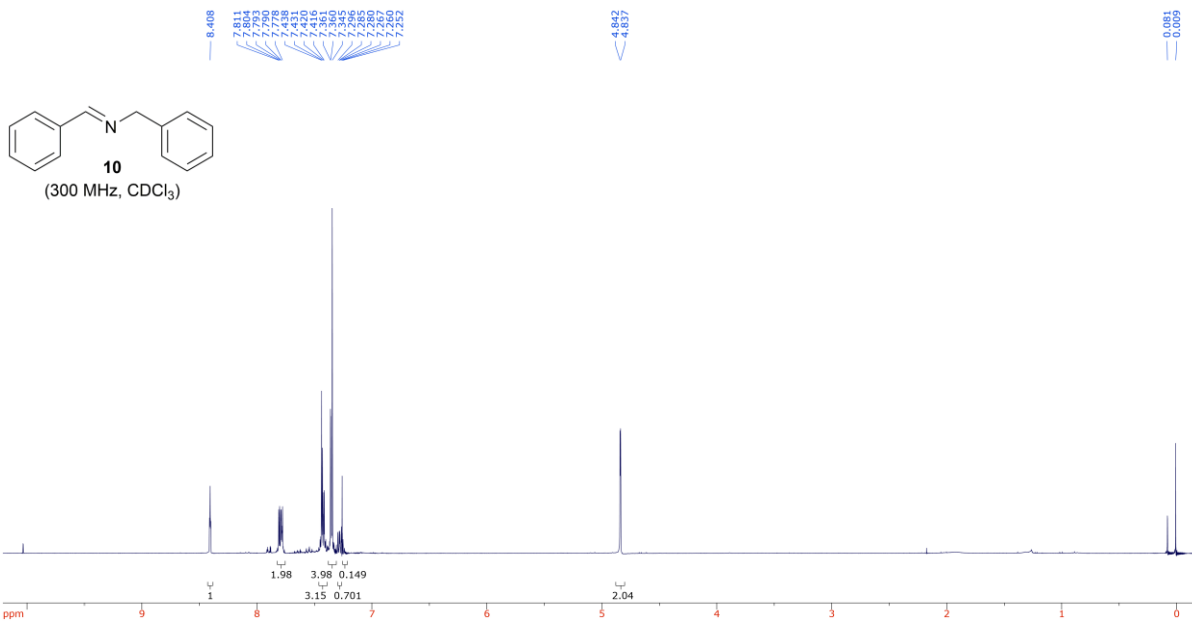




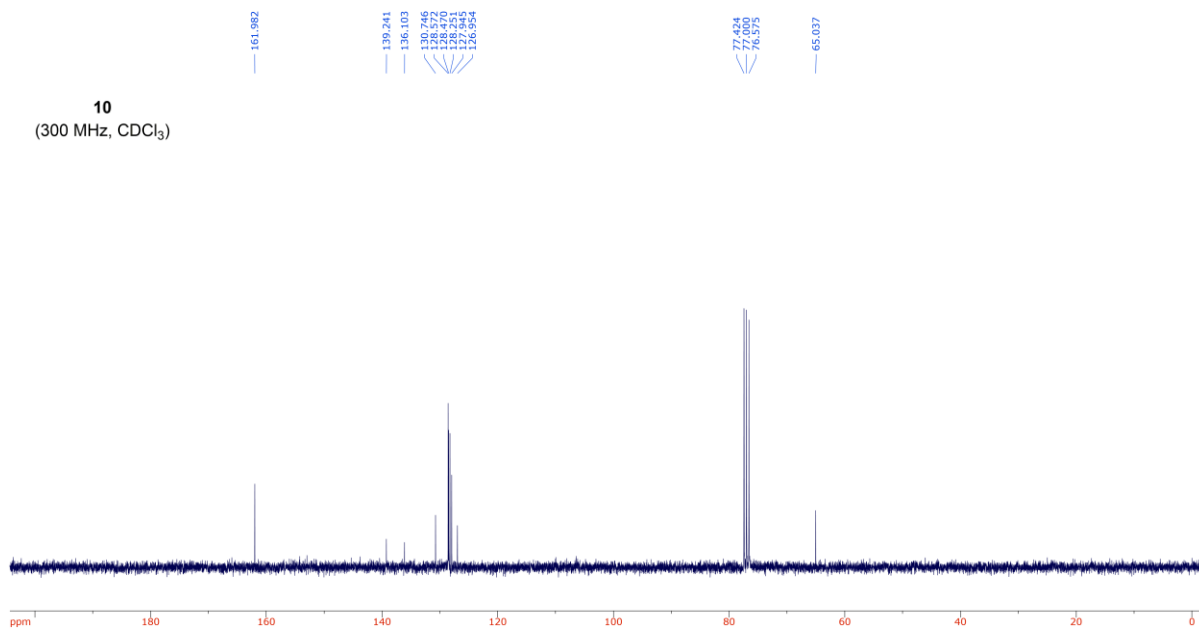
4
(75 MHz, CDCl₃)





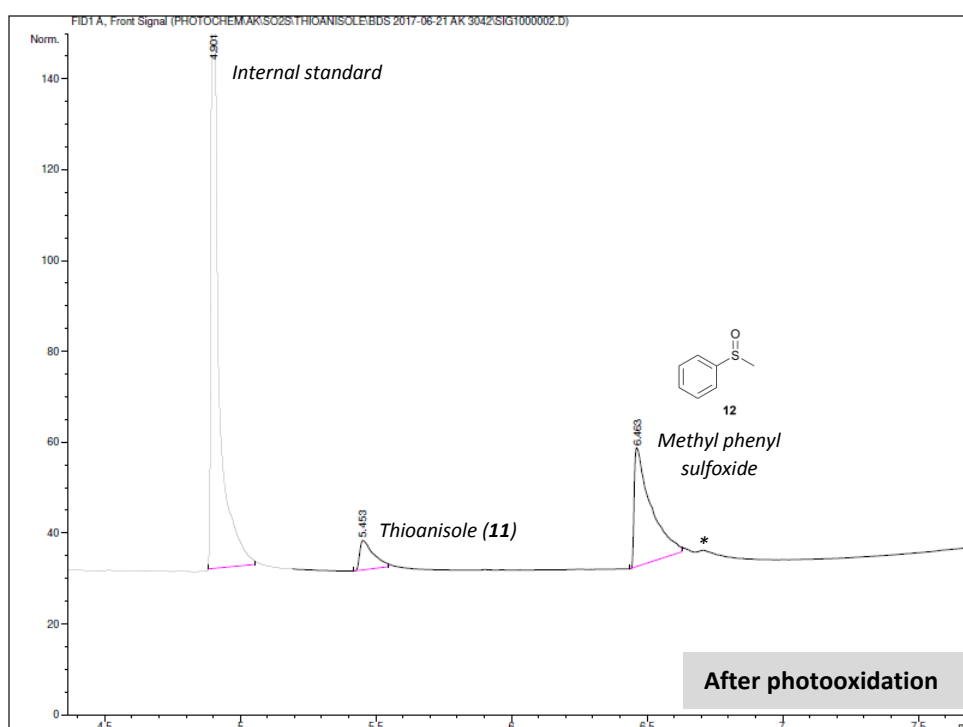
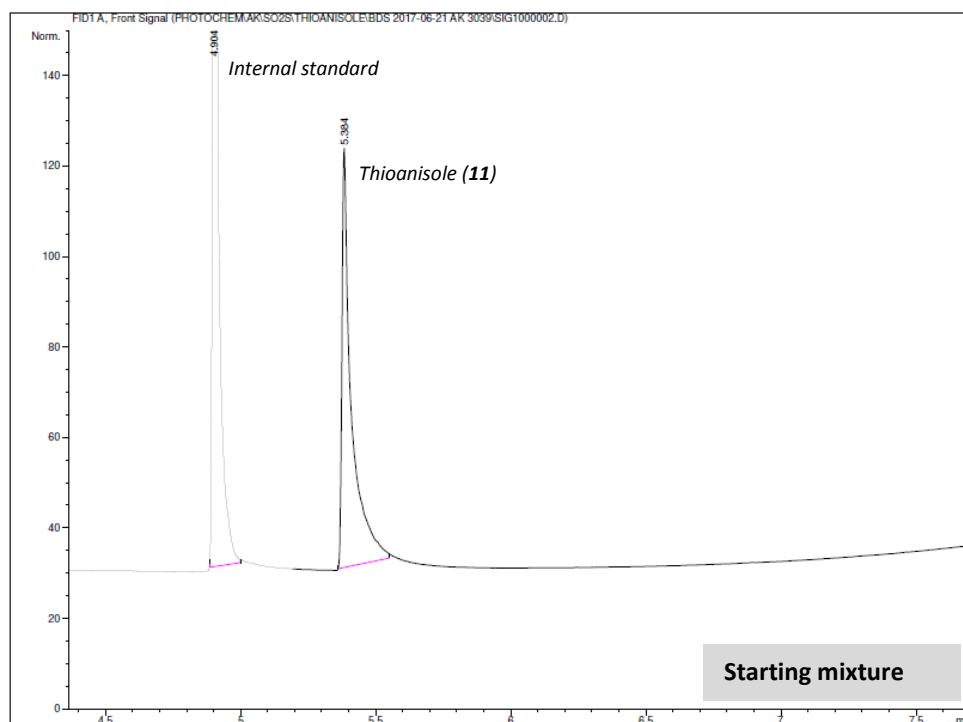


10
(300 MHz, CDCl₃)

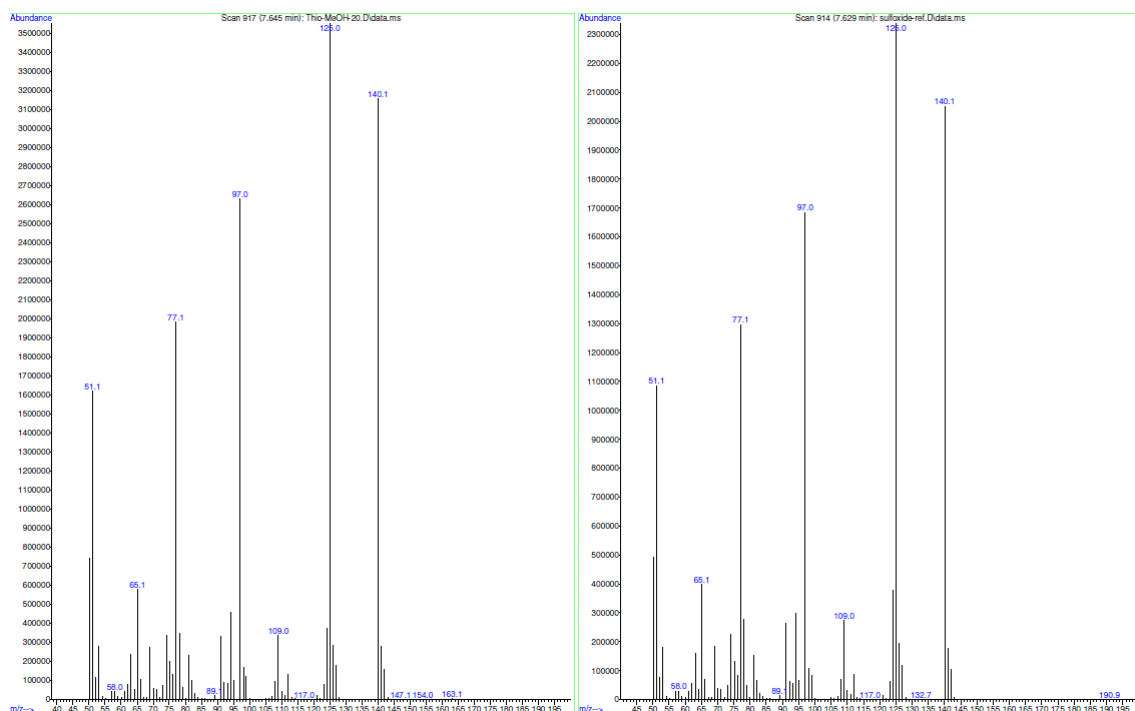


6. Chromatographic data

Photooxidation of thioanisole



GC-FID chromatograms are shown before (*upper panel*) and after photooxidation (*lower panel*) of thioanisole in the gas-liquid reactor system coupled to the photoreactor. Sulfoxide product **12** was characterized by comparison of retention time and mass spectrum (via GC-MS) with authentic methyl phenyl sulfoxide reference material (*see below*).

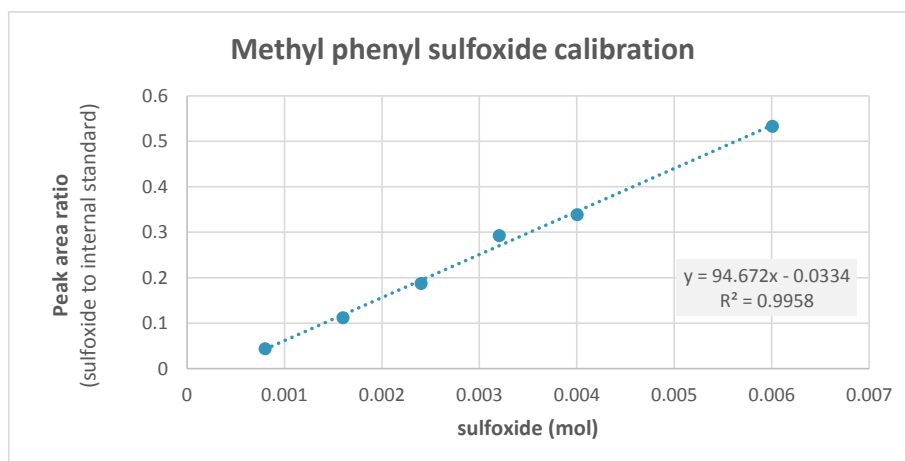


Electron impact mass spectra of the major product from thioanisole photooxidation (*left panel*) and of the sulfoxide **12** reference material (*right panel*).

A minor trace of methyl phenyl sulfone (MPS) was also detected (marked with asterisk in the chromatograms on p.16), but its presence was less than 1 % of **12** (molar ratio). The impurity level was determined by preparing reference mixtures, i.e. via spiking of minute, known quantities of MPS to **12**. After calculating peak area ratios in these mixtures (see Table S5), values were compared to the peak area ratio in the photoreaction mixture. This ratio of 66.8 corresponds to a MPS level of less than 1 mol%.

Table S5 Area ratios of **12** to methyl phenyl sulfone of a series of reference mixtures containing 1 %, 2.5 %, and 5 % methyl phenyl sulfone to **12** on a molar basis.

	mol% methyl phenyl sulfone	area ratio 12 : methyl phenyl sulfone
	1	66.7
<i>reference mixtures</i>	2.5	36.3
	5	12.3



Yield of **12** in the photooxidation mixture was determined by quantitative GC-FID analysis. Therefore, peak area ratio of **12** to internal standard in the reaction mixture was calculated and corresponding amount was determined from a linear calibration curve prepared using appropriate reference material.

GC-FID and GC-MS analysis were carried out as described under the General Information paragraph.

7. References

- ¹ M. Quaranta, M. Murkovic and I. Klimant, *Analyst*, 2013, **138**, 6243.
- ² K. N. Loponov, J. Lopes, M. Barlog, E. V. Astrova, A. V. Malkov and A. A. Lapkin, *Org. Process Res. Dev.*, 2014, **18**, 1443.
- ³ F. Lévesque and P. H. Seeberger, *Org. Lett.*, 2011, **13**, 5008.
- ⁴ G. I. Ioannou, T. Montagnon, D. Kalaitzakis, S. A. Pergantis and G. Vassilikogiannakis, *Chem. Photo Chem.*, 2017, **1**, 1.
- ⁵ J. H. Park, K. C. Ko, E. Kim, N. Park, J. H. Ko, D. H. Ryu, T. K. Ahn, J. Y. Lee and S. U. Son, *Org. Lett.*, 2012, **14**, 5502.